Inorg. Chem. **2004**, *43*, 3863–3870

Synthesis, Structural Characterization, Solution Chemistry, and Preliminary Biological Studies of the Ruthenium(III) Complexes [TzH][*trans*-$RuCl_4(Tz)_2$] and [TzH][*trans*-$RuCl_4$(DMSO)(Tz)]·(DMSO), the Thiazole Analogues of Antitumor ICR and NAMI-A

Pasquale Mura,*,† Mercedes Camalli,† Luigi Messori,*,‡ Francesca Piccioli,‡ Piero Zanello,§ and Maddalena Corsini§

Institute of Crystallography, Sezione di Monterotondo, Area della Ricerca di Roma, CNR CP10, I-00016 Monterotondo Stazione, Rome, Italy, Department of Chemistry, University of Florence, Via della Lastruccia 3, I-50019 Sesto Fiorentino, Florence, Italy, and Department of Chemistry, University of Siena, Via Aldo Moro, I-53100 Siena, Italy

Received December 9, 2003

Two ruthenium(III) complexes bearing the thiazole ligand, namely, thiazolium (bisthiazole) tetrachlororuthenate (**I**, TzICR) and thiazolium (thiazole, DMSO) tetrachlororuthenate (**II**, TzNAMI) were prepared and characterized. The crystal structures of both complexes were solved by X-ray diffraction methods and found to match closely those of the corresponding imidazole complexes. The behavior in aqueous solution of bothTzICR and TzNAMI was analyzed spectroscopically. The time-dependent spectrophotometric profiles resemble closely those of the related ICR and NAMI-A anticancer compounds, respectively. It is observed that replacement of imidazole with thiazole, a less basic ligand, produces a significant decrease of the ligand exchange rates in the case of the NAMI-like compound. The main electrochemical features of these ruthenium(III) thiazole complexes were determined and compared to those of ICR and NAMI-A. Moreover, some preliminary data were obtained on their biological properties. Notably, both complexes exhibit higher reactivity toward serum albumin than toward calf thymus DNA; cytotoxicity is negligible in line with expectations. A more extensive characterization of the pharmacological properties in vivo is presently in progress.

Introduction

Ruthenium(III) complexes have attracted large attention, in the last 20 years, as potential antitumor agents; some of them, indeed, exhibit very encouraging pharmacological profiles.[1] Following the clinical success of cisplatin, the first ruthenium(III) compounds to be tested as anticancer agents were developed by M. Clarke in the early 1980s. In 1987, Keppler reported the synthesis and structural characterization of [ImH][*trans*-$RuCl_4(Im)_2$], ICR, in a way the progenitor of a successful family of ruthenium(III) metallodrugs. ICR manifested interesting antitumor properties on animal models and inspired the synthesis of a number of related compounds of which the indazole analogue is the most important. In the following years, both ICR and its indazole analogue have been the object of extensive chemical and biological studies; the latter has recently entered phase I clinical trials.[2,3] At variance, the group of Alessio, Sava, and Mestroni in Trieste focused its attention on a series of ruthenium(III) compounds bearing DMSO as a ligand, the most popular of which is [ImH][*trans*-$RuCl_4$(DMSO)(Im)], NAMI-A. This latter compound is characterized by negligible cytotoxic effects and by outstanding antimetastatic properties, and is presently undergoing advanced phase I clinical trials.[4] Structure−function studies have demonstrated unambiguously that the biological activity of NAMI-A is strictly related to the

* Authors to whom correspondence should be addressed. P.M.: tel, +390690672615; fax, +390690672630; e-mail, Pasquale.Mura@ic.cnr.it. L.M.: tel, +390554573284; fax, +390554573385; e-mail, luigi.messori@unifi.it.

† Institute of Crystallography.

‡ University of Florence.

§ University of Siena.

(1) Clarke, M. J.; Zhu, F.; Frasca, D. R. *Chem. Rev.* **1999**, *99* (9), 2511.

(2) Lipponer, K. G.; Vogel, E.; Keppler, B. K. *Met.-Based Drugs* **1996**, *3*, 243.

(3) Kung, A.; Piper, T.; Wissiack, R.; E. Rosemberg, E.; B. K. Keppler, B. K. *J. Biol. Inorg. Chem.* **2001**, *6* (3), 292.

(4) Sava, G.; Alessio, E.; Bergamo, A.; Mestroni, G. *Top. Biol. Inorg. Chem.* **1999**, *1*, 143.

10.1021/ic0354116 CCC: $27.50
Published on Web 05/29/2004

progressive release of one or more of its chloride ligands; in fact, more inert analogues of NAMI-A such as the rhodium(III) and iridium(III) complexes turned out to be devoid of biological activity.[5,6] Yet, the effective molecular mechanism of action and the final targets for NAMI-A have not been identified, although several hypotheses have been suggested.[4,7] For instance, it is yet not clear whether the ruthenium(III) center undergoes reduction upon reaction with biomolecules, as stated by the classical "activation by reduction" hypothesis. Moreover, it is not proved that these compounds exert their action through a direct interaction with DNA as in the case of classical platinum(II) complexes,[8] although some increased concentration of ruthenium in the cell nucleus has been reported.

Noticeably, a marked reactivity of ruthenium(III) complexes with plasma proteins has been described.[9−13] In addition, ruthenium(III) complexes were recently shown to act as potent antiangiogenic agents and nitric oxide scavengers;[14] these activities might be somehow related to the important antimetastatic effects.

In the search for novel ruthenium(III) complexes with better pharmacological profiles, Alessio and Sava recently showed that the pyrazole, thiazole, and pyrazine analogues of NAMI-A manifest interesting pharmacological properties and might provide some improvements compared to the reference compounds.[15]

Prompted by these observations, we report here an extensive chemical characterization of the thiazole analogues of both ICR and NAMI-A. The specific issue we want to address with the present investigation is the accurate description of the consequences of the imidazole/thiazole replacement on both the redox and the kinetic properties of these ruthenium(III) complexes; in addition, we have measured the cytotoxic properties of these thiazole complexes and analyzed their reactivity against calf thymus DNA and bovine serum albumin. In our opinion, the present results provide some further insight into the structure−function relationships of this new class of antitumor compounds.

Experimental Section

Materials. All starting materials (apart from complex $[(DMSO)_2H][trans\text{-}RuCl_4(DMSO)_2]$, prepared as described in the literature)[16] and solvents were commercially available. The syntheses were carried out under nitrogen. Infrared spectra were recorded on a Perkin-Elmer 16PC FTIR spectrophotometer.

Bovine serum albumin and calf thymus DNA were purchased from SIGMA Chemical Company. Where not differently stated, experiments were performed in phosphate buffer containing NaH_2PO_4 (50 mM), NaCl (100 mM), (pH 7.4).

Synthesis of [TzH][*trans*-RuCl$_4$(Tz)$_2$] (I, ICR). $RuCl_3 \cdot H_2O$ (0.21 g, 1 mmol) was dissolved in 2.5 mL of ethanol and 2.5 mL of HCl 1 N and gently refluxed for 1 h 30 min (oil bath temperature 95 °C). After the mother liquor was cooled at room temperature, 0.48 g (0.40 mL, 5.6 mmol) of thiazole, dissolved in 0.5 mL of ethanol and 0.5 mL of HCl 6 N, was added with stirring. The mixture was gently refluxed for 30 min (oil bath temperature 80 °C).[17] A good quantity of precipitate formed. The brown-red microcrystals were filtered off, washed with ethanol and ether, and dried in a vacuum. Yield: 0.31 g (62%). Anal. Calcd for $C_9H_{10}Cl_4N_3RuS_3$ (M = 499.27): C, 21.64; H, 2.02; N, 8.45; S, 19.26. Found: C, 21.70; H, 1.85; N, 8.31; S, 19.17. An IR band at 250.0 (ms) cm^{-1} is tentatively attributed to ν_{Ru-N}.[18]

Synthesis of [TzH][*trans*-RuCl$_4$(DMSO)(Tz)]·(DMSO) (II, TzNAMI). $[(DMSO)_2H][trans\text{-}RuCl_4(DMSO)_2]$[16] (0.1 g, 0.18 mmol) was suspended in 2 mL of DMSO/acetone mixture. Afterward, 0.046 g of thiazole (0.038 mL, 0.54 mmol), dissolved in 0.5 mL of DMSO/acetone mixture, was added with stirring. In a few minutes the suspension became a clear yellow-orange solution. After several minutes of stirring, ether was added to the mother solution until incipient precipitation. The reaction mixture was left overnight. A good quantity of nice clear orange-yellow crystals formed. The crystals were filtered off, washed with ethanol/ether mixture, and dried in a vacuum. Yield: 0.092 g (95%). Anal. Calcd for $C_{10}H_{19}Cl_4N_2O_2RuS_4$ (M = 570.41): C, 21.05; H, 3.36; N, 4.91; S, 22.48. Found: C, 21.08; H,3.40; N, 4.97; S, 22.30. An IR band at 244.0 (mw) cm^{-1} is tentatively attributed to ν_{Ru-N}.[18]

X-ray Structure Solution and Refinement of [TzH][*trans*-RuCl$_4$(Tz)$_2$] (I, TzICR) and [TzH][*trans*-RuCl$_4$(DMSO)(Tz)]·(DMSO) (II, TzNAMI). Brown-red crystals of **I** and orange-yellow crystals of **II** were obtained from the mother liquor of the reaction. Data collections were performed using a Rigaku AFC5 diffractometer (room temperature); no decay correction was applied. Data were corrected for Lorentz and polarization effects. An empirical absorption correction, based on azimuthal scans of several reflections, was applied to intensities.[19] The structures were solved using

(5) Marcon, G.; Casini, A.; Mura, P.; Messori, L.; Bergamo A.; Orioli, P. *Met.-Based Drugs* **2000**, *7*, 195 and references therein.
(6) (a) Messori, L.; Marcon, G.; Orioli, P.; Fontani, M.; Zanello, P.; Bergamo, A.; Sava, G.; Mura, P. *J. Inorg. Biochem.* **2003**, *95*, 37 and references therein. (b) Mura, P.; Casini, A.; Marcon, G.; Messori, L. *Inorg. Chim. Acta* **2001**, *312*, 74 and references therein.
(7) Sava, G.; Capozzi, I.; Bergamo, A.; Gagliardi, R.; Cocchietto, M.; Masiero, L.; Onisto, M.; Alessio, E.; Mestroni, G.; Garbisa, S. *Int. J. Cancer* **1996**, *68* (1), 60.
(8) Gallori, E.; Vettori, C.; Alessio, E.; Gonzalez, F.; Vilchez, Vilaplana, R.; Orioli, P.; Messori, L.; Casini, A. *Arch. Biochem. Biophys.* **2000**, *376* (1), 156.
(9) Kratz, F.; Hartmann, M.; Messori, L. *J. Biol. Chem.* **1994**, *269*, 2581.
(10) Kratz, F.; Keppler, B. K.; Hartmann, M.; Messori, L.; Berger, M. R. *Met.-Based Drugs* **1996**, *3*, 15.
(11) Kratz, F.; Keppler, B. K.; Messori, L.; Smith, C.; Baker, E. N. *Met.-Based Drugs* **1994**, *1*, 169.
(12) Messori, L.; Orioli, P.; Vullo, D.; Alessio, E.; Iengo, E. *Eur. J. Biochem.* **2000**, *267* (4), 1206.
(13) Trynda-Lemiesz, L.; Keppler, B. K.; Kozłowski, H. *J. Inorg. Biochem.* **1999**, *73* (3), 123.
(14) Morbidelli, L.; Donnini, S.; Filippi, S.; Messori, L.; Piccioli, F.; Orioli, P.; Sava, G.; Ziche, M. *Br. J. Cancer* **2003**, *88*, 1484.
(15) Bergamo, A.; Gava, B.; Alessio, E.; Mestroni, G.; Serli, B.; Cocchietto, M.; Zorzet, S.; Sava, G. *Int. J. Oncol.* **2002**, *21*, 1331.
(16) Alessio, E.; Balducci, G.; Calligaris, M.; Costa, G.; Attia, W. M.; Mestroni, G. *Inorg. Chem.* **1991**, *30*, 609.
(17) On performing the reaction at room temperature (see ref 18 , B. K. Keppler and co-workers), compound **I** is obtained from the mother liquor in two different crystalline modification, red-brown crystals and beige-gold thin plates. The elemental analyses of both forms are the same and in perfect agreement with the formula proposed for **I**; the same holds for the infrared spectra, ^{1}H NMR spectra, and X-ray powder spectra. Single-crystal analyses, of both crystalline modifications, reveal an identical stereochemistry; the unique difference observed is a more pronounced disorder in the thiazole rings for the beige-gold modification; see discussion for compound **I**.
(18) Keppler, B. K.; Rupp, W.; Juhl, U. M.; Endres, H.; Niebl, R.; Balzer, W. *Inorg. Chem.* **1987**, *26*, 4366.
(19) Molecular Structure Corporation (1985). TEXSAN TEXRAY, Structure Analysis Package. MSC, 3200 Research Forest Drive, The Woodlands, TX 77381.

Table 1. Crystal Data for [TzH][*trans*-$RuCl_4(Tz)_2$] and [TzH][*trans*-$RuCl_4$(DMSO)(Tz)]·(DMSO)

	[TzH][*trans*-$RuCl_4(Tz)_2$], (**I**, TzICR)	[(TzH][*trans*-$RuCl_4$-(DMSO)(Tz)]·(DMSO) (**II**, TzNAMI)
formula	$C_9H_{10}Cl_4N_3RuS_3$	$C_{10}H_{19}Cl_4N_2O_2RuS_4$
MW	499.27	570.41
crystal dimens (mm)	0.19 × 0.14 × 0.12	0.18 × 0.12 × 0.10
crystal system	monoclinic	triclinic
space group	$P2_1/n$	$P\bar{1}$
cell dimens	*a*	*b*
a (Å)	7.594(7)	7.676(2)
b (Å)	21.348(7)	8.694(2)
c (Å)	10.133(2)	15.866(4)
α (deg)		80.02(2)
β (deg)	96.32(4)	87.45(2)
γ (deg)		84.55(2)
V (Å^3)	1633(2)	1037.7(5)
Z	4	2
calcd density (g cm^{-3})	2.032	1.826
scan method	*ω*/2*θ*	*ω*/2*θ*
radiation	Cu Kα (*λ* = 1.54178 Å)	Cu Kα (*λ* = 1.54178 Å)
monochromator	graphite crystal	graphite crystal
2*θ* range (deg)	5−124	5−124
octants collected	*h*, *k*, ±*l*	±*h*, ±*k*, ±*l*
total no. of data	2575	6516
variable scan speed range (deg min^{-1})	4−16	4−16
no. of obsd data ($I_o > 3\sigma(I_o)$)	1727	2776
R value for equiv reflns	0.056	0.076
μ (mm^{-1})	17.465	14.758
F(000)	980	570
final residuals:	(for 1727 data)	(for 2776 data)
R, R_w[c]	0.057, 0.076	0.048, 0.068
a, *b*, *c* values in the weight function $W = 1.0/(a + bF_o + cF_o^2)$	2.9002, 0.1291, 0.0017	0.5996, 0.1462, 0.002
GOF for last cycle	0.95	0.91
max Δ/*σ* for last cycle	0.03	0.00

[a] Lattice parameters calculated from 25 high-angle reflections measured at ±2*θ* (2*θ* interval 35.64−47.99°). [b] Lattice parameters calculated from 25 high-angle reflections measured at ±2*θ* (2*θ* interval 30.92−44.86°).[c] $R = \sum||F_o| - |F_c||/\sum|F_o|$; $R_w = [\sum w(|F_o| - |F_c|)^2/\sum w|F_o|^2]^{1/2}$.

SIR97 program[20] and refined as full matrix in the least-squares calculation using CAOS programs.[21] The number of observations for **I** (TzICR) was 1727 ($I_o > 3\sigma(I_o)$), and the number of variable parameters was 181 (9.5 observations for each parameter). The full matrix refinement gave $R = 0.057$ and $R_w = 0.076$; considering the disorder present in the structure, see discussion, concerning thiazoles rings, we decided not to introduce the calculated contribution of the hydrogen atoms. Additional details of the crystallographic experiment concerning **I** are given in Table 1.

The number of observations for **II** (TzNAMI) was 2776 ($I_o > 3\sigma(I_o)$), and the number of variable parameters was 208 (13.3 observations for each parameter). The full matrix refinement, after introduction of the fixed contribution of 19 H atoms of the thiazole and DMSO, gave $R = 0.048$ and $R_w = 0.068$. Additional details of the crystallographic experiments concerning **II** are given in Table 1.

Spectroscopic Measurements. The solution behavior of TzICR and TzNAMI was analyzed by monitoring the electronic spectra of freshly prepared solutions over a 24 h period. The concentration of the two complexes for spectrophotometric determinations was 1×10^{-4} M.

The interactions of TzICR and TzNAMI with serum albumin and calf thymus DNA were studied by UV−vis spectroscopy, the concentration of the ruthenium(III) complexes was 1×10^{-4} M, and the molar ratios toward these biomolecules were 1:1 in the reference buffer.

Visible absorption spectra were carried out with a Perkin-Elmer Lambda Bio 20 instrument. The measurements were done at room temperature (25 °C).

Ultrafiltration Experiments. The ruthenium/protein and ruthenium/DNA adducts were repeatedly ultrafiltrated after 24 h incubation at room temperature, using Centricon YM-10 (Amicon Bioseparations, Millipore Corporation). The absorption spectra of the upper and the lower portions were recorded.

ESI-MS. The concentration of the two complexes for ESI-MS measurements was 1×10^{-3} M in H_2O, and the ESI-MS spectra were recorded at $t = 0$ using a Thermo Finnigan LCQ Deca XP plus instrument.

Electrochemistry. Materials and apparatus for electrochemistry have been described elsewhere.[22] All potential values are referred to the saturated calomel electrode (SCE).

Cell Culture and Cytotoxicity Assay. In vitro cytotoxicity assays on cultured human tumor cell lines still represent the standard method for the initial screening of antitumor agents. Thus, as a first step for their pharmacological evaluation, the two ruthenium complexes were assayed toward the ovarian carcinoma A2780/S human cell line.

This cell line was cultured in RPMI 1640 medium supplemented with fetal bovine serum (FBS) and antibiotics (streptomycin 100 mg/mL and penicillin 100 U/mL) at 37 °C in a 5% CO_2 atmosphere and subcultured twice weekly. Experiments were conducted on exponentially growing cells. Drugs were dissolved in sterile DMSO. Inhibition of cell growth was determined after a 72 h drug exposure by the Sulphorhodamine B (SRB) assay performed in 96-well plates, using RPMI 1640 medium+ 5% FBS, according to the protocol of Skehan.[23]

Results

Preparation, Characterization and Molecular Structure of [TzH][*trans*-$RuCl_4(Tz)_2$] (I, TzICR). Complex **I** was obtained by a modified procedure with respect to the method reported by Keppler and co-workers.[17,18] The infrared spectra of **I** show a band at 326.0 (s) cm^{-1} attributed to Ru−Cl stretching vibrations. Elemental analyses confirmed the obtainment of the desired compound.

Figure 1 shows a perspective view of **I** and defines the atom numbering scheme for the heavy atoms. Selected bond lengths and angles are given in Table 2. Crystallographic data in CIF format is available as Supporting Information.

As expected, the ruthenium(III) ion is hexacoordinated with the four chlorides in the equatorial plane and the two thiazole ligands in axial position. The same coordination was previously observed for [ImH][*trans*-$RuCl_4(Im)_2$] (ICR).[18] Notably the substitution of imidazole with thiazole disrupts the crystal symmetry present in ICR.[18] Moreover complex **I** shows disorder regarding the two coordinated thiazoles and

(20) Altomare, A.; Burla, M. C.; Camalli, M.; Cascarano, G. L.; Giacovazzo, C.; Guagliardi, A.; Moliterni, A. G. G.; Polidori, G.; Spagna, R. *J. Appl. Crystallogr.* **1999**, *32*, 115.
(21) Camalli, M.; Spagna, R. *J. Appl. Crystallogr.* **1994**, *27*, 861.
(22) Fabrizi de Biani, A. F.; Laschi, F.; Zanello, P.; Fergusson, G.; Trotter, J.; O'Riordan, G. M.; Spalding, T. R. J. *J. Chem. Soc., Dalton Trans.* **2001**, 1520.
(23) Skehan, P.; Storeng, R.; Scudiero, D.; Monks, A.; McMahon, J.; Vistica, D.; Warren, J. T.; Bokesh, H.; Kenney, S.; Boyd, M. R. J. *J. Natl. Cancer Inst.* **1990**, *82*, 1107.

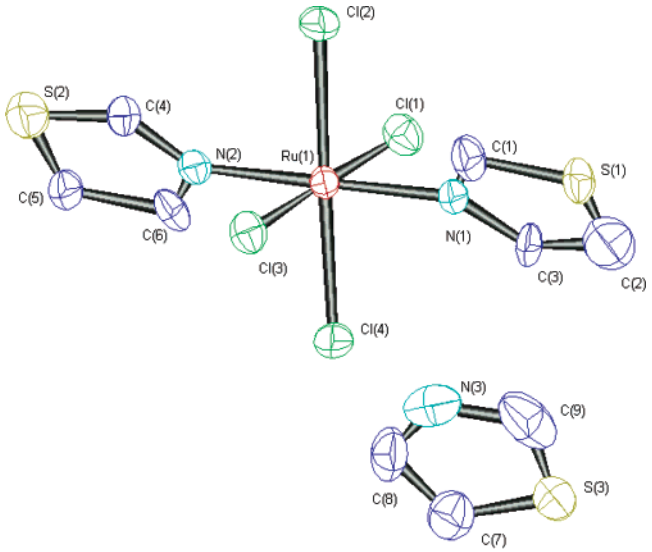

Figure 1. Geometry[21] of compound **I** (TzICR). Thermal ellipsoids are drawn at the 50% probability level. Due to the disorder (see discussion) in the thiazole rings, the fixed contribution of the H atoms was not introduced.

Table 2. Selected Bond Lengths (Å) and Angles (deg) for [TzH][*trans*-$RuCl_4(Tz)_2$] (**I**, TzICR)

Ru(1)		Cl(1)	2.352(3)	Ru(1)		Cl(4)	2.357(3)
Ru(1)		Cl(2)	2.355(3)	Ru(1)		N(1)	2.086(8)
Ru(1)		Cl(3)	2.345(3)	Ru(1)		N(2)	2.081(9)
Cl(4)	Ru(1)	Cl(1)	89.8(1)	Cl(3)	Ru(1)	Cl(2)	91.9(1)
Cl(2)	Ru(1)	Cl(1)	88.9(1)	Cl(3)	Ru(1)	N(1)	89.1(2)
Cl(2)	Ru(1)	Cl(4)	178.4(1)	N(2)	Ru(1)	Cl(1)	90.4(2)
N(1)	Ru(1)	Cl(1)	90.2(2)	N(2)	Ru(1)	Cl(4)	90.4(2)
N(1)	Ru(1)	Cl(4)	90.2(8)	N(2)	Ru(1)	Cl(2)	90.4(2)
N(1)	Ru(1)	Cl(2)	89.1(2)	N(2)	Ru(1)	N(1)	179.2(4)
Cl(3)	Ru(1)	Cl(1)	178.9(1)	N(2)	Ru(1)	Cl(3)	90.3(2)
Cl(3)	Ru(1)	Cl(4)	89.5(1)				

in the thiazolium ion. The refinement of the model obtained from the direct method solution shows distorted thiazole rings, with high isotropic thermal values. A careful check of the final difference Fourier map does not produce alternative positions. At this stage we assumed for the two coordinated thiazole rings a statistic 2-fold-like disorder around the Ru−N vector, and for the thiazolium ring a statistic 5-fold-like disorder around a vector perpendicular to it, considering that carbon and nitrogen are indistinguishable. Refinement of the occupation site factor, with the above assumptions, gives a distribution for the S(1)−C(1)−N(1)−C(3)−C(2) ring 78% and 22%, for the S(2)−C(4)−N(2)−C(6)−C(5) ring 61% and 39%; for the S(3)−C(9)−N(3)−C(8)−C(7) ring only three positions are detected, the first with the S atom in the site called S(3) with 19% of occupancy, the second with the S atom in the site called C(9), 29%, and the last with the S atom in the position called C(7), 52%. Refinement of this model gives a discrepancy factor of $R = 0.057$ and $R_w = 0.076$.[21] The obtained bond distances of the thiazole rings are comparable to that of the complex **II** (TzNAMI), considering the standard deviations, apart from the C(5)−C(6) distance, see CIF. The crystal packing of the complex **I** does not give any information on the disorder. The Ru−Cl distances in **I** (mean value Ru−Cl = 2.352(3) Å) and those of ICR (mean value Ru−Cl = 2.349(1) Å) are almost the same;[18] the same holds for Ru−N = 2.083(8) Å in **I** (mean value) and Ru−N = 2.079(3) Å in ICR. The plane of the two coordinated trans thiazoles are quasi parallel (4.2°) in **I** instead of nearly perpendicular in ICR (84°).[18] The calculated X-ray powder spectrum of **I** perfectly matches the experimental X-ray powder spectra obtained by **I** microcrystals.

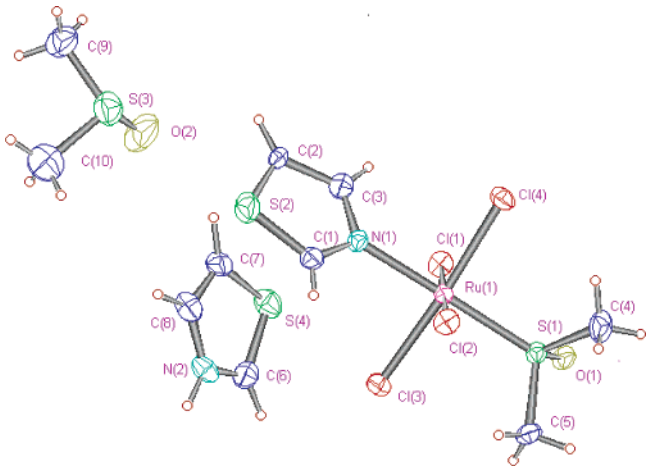

Figure 2. Geometry[21] of compound **II** (TzNAMI). Thermal ellipsoids are drawn at the 50% probability level.

Table 3. Selected Bond Lenghts (Å) and Angles (°) for [(TzH][*trans*-$RuCl_4$(DMSO)(Tz)]. (DMSO), (**II**, TzNAMI)

Ru(1)		Cl(1)	2.360(2)	Ru(1)		Cl(4)	2.358(2)
Ru(1)		Cl(2)	2.345(2)	Ru(1)		S(1)	2.287(1)
Ru(1)		Cl(3)	2.349(2)	Ru(1)		N(1)	2.105(4)
Cl(4)	Ru(1)	Cl(1)	88.85(6)	Cl(3)	Ru(1)	Cl(2)	90.92(6)
Cl(2)	Ru(1)	C1(1)	179.10(6)	Cl(3)	Ru(1)	S(1)	91.63(5)
Cl(2)	Ru(1)	Cl(4)	90.43(6)	N(1)	Ru(1)	Cl(1)	89.0(1)
S(1)	Ru(1)	Cl(1)	92.02(5)	N(1)	Ru(1)	Cl(4)	88.4(1)
S(1)	Ru(1)	Cl(4)	92.06(5)	N(1)	Ru(1)	Cl(2)	90.4(1)
S(1)	Ru(1)	Cl(2)	88.54(5)	N(1)	Ru(1)	S(1)	178.8(1)
Cl(3)	Ru(1)	Cl(1)	89.77(6)	N(1)	Ru(1)	Cl(3)	87.9(1)
Cl(3)	Ru(1)	Cl(4)	176.10(5)				

Preparation, Characterization and Molecular Structure of [TzH][*trans*-$RuCl_4$(DMSO)(Tz)]·(DMSO) (II, TzNAMI). Compound **II** was prepared with the same procedure reported in the literature for NAMI-A.[4] The infrared spectra of **II** show two bands at 346.0 (ms) and 330.0 (ms) cm^{-1} attributed to Ru−Cl stretching vibrations. Elemental analyses confirmed the obtainment of the desired compound.

Figure 2 shows a perspective view of **II** and defines the atom numbering scheme for the heavy atoms. Selected bond lengths and angles are given in Table 3. Crystallographic data in CIF format is available as Supporting Information. As expected the Ru(III) ion is hexacoordinated, with the four chlorine atoms in equatorial position and the DMSO and thiazole ligands in axial position.

The crystal structure of NAMI-A was not reported[4] but only that of NAMI, i.e., [Na][*trans*-$RuCl_4$(DMSO)(Im)]·H_2O, Me_2CO.[24] In any case comparison of the geometry of the two anions is possible. The Ru−Cl distance in **II** (mean value Ru−Cl = 2.353(2) Å) and those of NAMI (mean value Ru−Cl = 2.342(1) Å)[24] are comparable and close to the average

(24) Alessio, E.; Balducci, G.; Lutman, A.; Mestroni, G.; Calligaris, M.; Attia, W. M. *Inorg. Chim. Acta* **1993**, *203*, 205 and references therein.

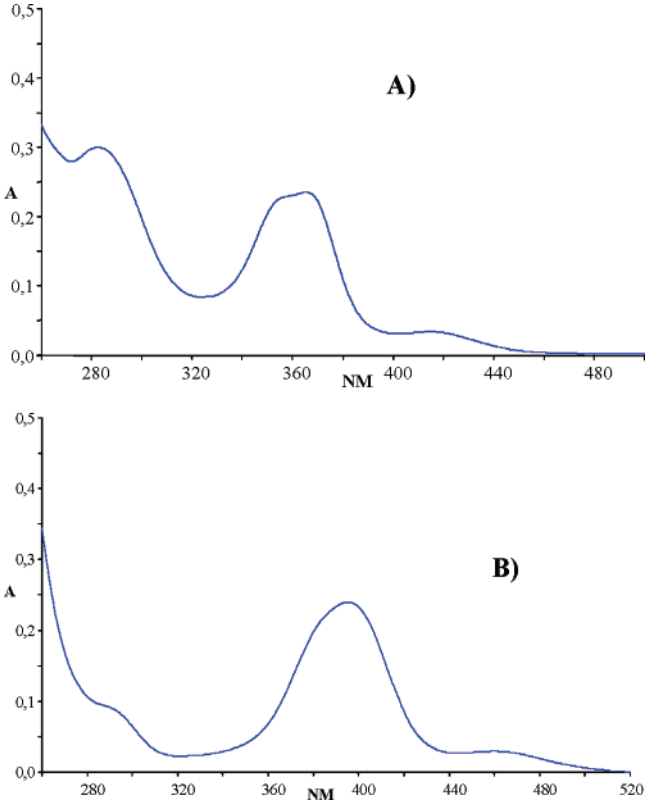

Figure 3. Electronic spectra of **I** (TzICR) (A) and **II** (TzNAMI) (B) in water; the concentration of each complex is 1×10^{-4} M.

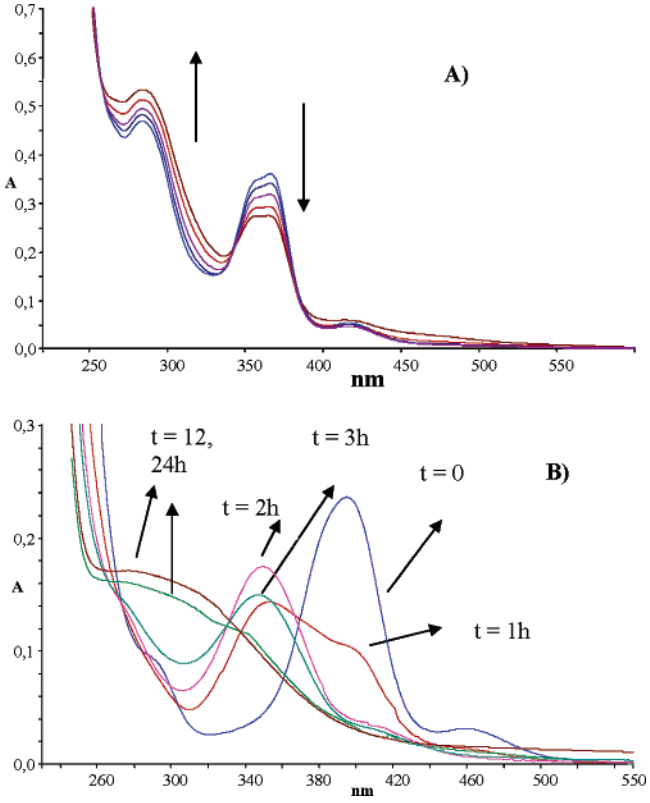

Figure 4. Hydrolysis profiles of **I** (TzICR) (A) in the reference buffer pH 7.4 (t = 0, 3, 6, 12, and 24 h; concentration of the complex is 1×10^{-4} M) and of **II** (TzNAMI) (B) under the same experimental conditions.

value of 2.249(8) Å found in related compounds.[25] The Ru−N distance in **II** (2.105(4) Å) is similar to that found for NAMI (2.081(2) Å)[24] and in **I** (mean value 2.083(8) Å) considering the standard deviations; the same holds for the Ru−S = 2.287(1) Å in **II** and Ru−S = 2.296(1) Å in NAMI.[25]

Solution Studies. Both ruthenium(III) thiazole complexes are acceptably soluble in water. Solutions of either **I** (TzICR) or **II** (TzNAMI) are characterized by relatively intense bands that are classically assigned as LMCT bands. The respective spectra are shown in Figure 3. Notably compound **I** shows two intense bands at 280 ($\epsilon \sim 3000$ cm^{-1} M^{-1}) and 360 nm ($\epsilon \sim 2400$ cm^{-1} M^{-1}) (with a shoulder at 430 nm), whereas compound **II** exhibits a main band at 390 nm ($\epsilon \sim 2400$ cm^{-1} M^{-1}) with a shoulder at 430 nm and a second band at 290 nm ($\epsilon \sim 2500$ cm^{-1} M^{-1}). Notably these spectral features resemble closely those of ICR (λ_{max} at 350 nm, $\epsilon \sim 3200$ cm^{-1} M^{-1}) and NAMI-A (λ_{max} at 400 nm, $\epsilon \sim 3600$ cm^{-1} M^{-1}).

The visible spectra of either compound, in water, do not show any major change when monitored over a few hours. However, over larger time intervals, significant spectral changes are observed (specifically a pronounced decrease of the main visible band), that are ascribed to the progressive hydrolysis of the coordinated chlorides. ESI-MS spectra of freshly prepared solutions of both ruthenium(III) complexes were recorded. A molecular peak at m/z 342 corresponding to [$RuCl_2(Tz)_2$], in the case of TzICR, and one at m/z 337, corresponding to [$RuCl_2$(DMSO)(Tz)] in the case of TzNAMI, were observed.

As found for ICR and NAMI-A, hydrolysis is much faster when the compounds are dissolved within a physiological buffer at pH 7.4. Characteristic spectral patterns for the two complexes dissolved in the buffer are reported in Figure 4A,B.

Compound **I** (TzICR) shows a slow, progressive decrease in intensity of the band located at 360 nm and the concomitant increase of a band at 280 nm. A clear isosbestic point is appreciated at 340 nm, indicating an equilibrium between two species. By analogy with the case of ICR, we interpret this spectral pattern in terms of the progressive release of a coordinated chloride and of its replacement by a water molecule. The half-life for the disappearance of the main visible band is around 6 h, to be compared with a similar value measured for ICR. In other words, replacement of imidazole by thiazole does not affect importantly the kinetics of chloride release.

The hydrolysis profile of compound **II** (TzNAMI) is reported in Figure 4B. Typically, the hydrolysis process is much faster for this complex than for TzICR; this means that the replacement of a thiazole group with DMSO results into some significant acceleration of the release of the first chloride. Noticeably, the overall spectral pattern of hydrolysis is very similar to that described for NAMI-A. In fact, the main visible band of the starting compound is replaced, within ~2 h, by a band centered at 360 nm. In turn, the latter band starts decreasing and is replaced, within 12 h, by

(25) Calligaris, M.; Bresciani-Pahor, N.; Srivastava, R. S. *Acta Crystallogr.* **1993**, *49*, 448 and references therein.

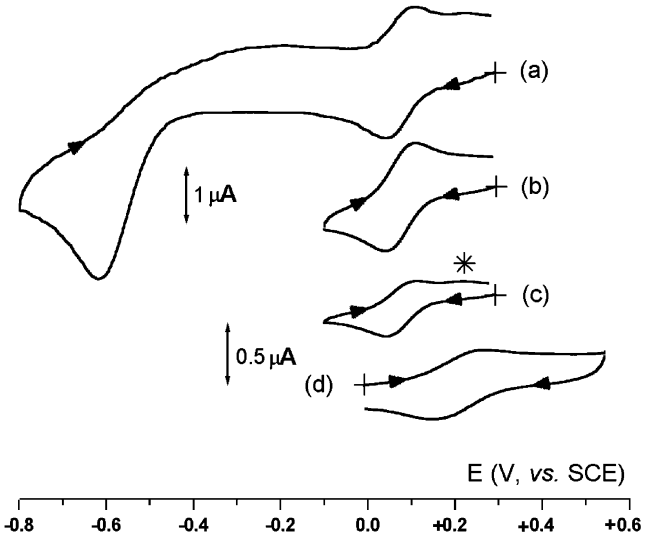

Figure 5. Cyclic voltammetric responses recorded at a platinum electrode in an aqueous solution of [TzH][$RuCl_4$(DMSO)(Tz)](DMSO) (0.4×10^{-3} mol dm^{-3}) (a−c). (d) After exhaustive one-electron reduction (see text). NaCl (0.2 mol dm^{-3}) supporting electrolyte. Scan rates: (a, b, d) 0.2 V s^{-1}; (c) 0.02 V s^{-1}.

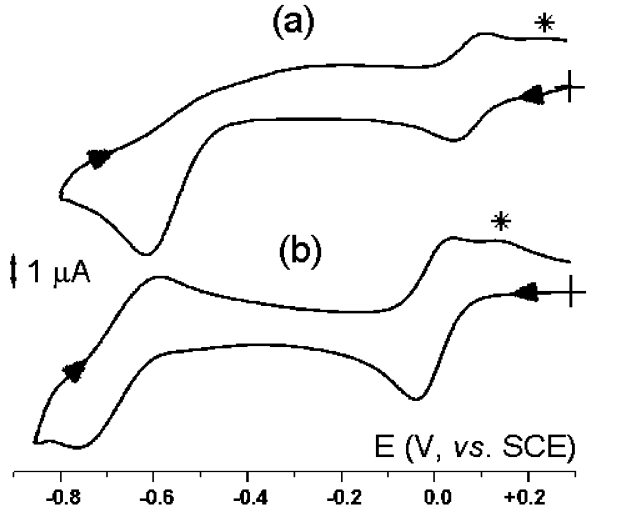

Figure 6. Cyclic voltammetric responses recorded at a platinum electrode in aqueous solutions of [TzH][$RuCl_4$(DMSO)(Tz)](DMSO) (0.4×10^{-3} mol dm^{-3}) (a) and [ImH][$RuCl_4$(DMSO)(Im)] (1.1×10^{-3} mol dm^{-3}) (b), respectively. NaCl (0.2 mol dm^{-3}) supporting electrolyte. Scan rate 0.2 V s^{-1}.

another band centered at 300 nm. The half-life for the first process (the decrease of the band centered at 400 nm) is about 75 min, thus significantly larger than that measured for NAMI-A (∼30 min) under the same experimental conditions. This means that replacement of imidazole with the less basic thiazole ligand results in kinetic stabilization of the ruthenium(III) complex in line with recent observations.[14] In any case, it is proved that the presence of a DMSO ligand coordinated to the ruthenium(III) center renders the hydrolysis processes faster.

Electrochemistry. Figure 5 shows the cyclic voltammetric behavior of the monoanion [$RuCl_4$(DMSO)(Tz)]$^-$ in aqueous solution. It displays two successive reduction processes, the first of which exhibits features of chemical reversibility in the cyclic voltammetric time scale, as shown in Figure 5a,b. Since controlled potential coulometry corresponding to the first reduction ($E_w = -0.1$ V) consumed one electron per molecule, we assign it to the redox process [$Ru^{III}Cl_4$(DMSO)(Tz)]$^-$/[$Ru^{II}Cl_4$(DMSO)(Tz)]$^{2-}$. In reality, analysis[26] of the pertinent cyclic voltammograms with scan rate varying from 0.02 to 1.0 V s^{-1} indicates that the electrogenerated Ru(II) complex is not indefinitely stable, in that while the current function $i_{pc}v^{-1/2}$ remains constant, the current ratio i_{pa}/i_{pc}, which is about 1.0 at the highest scan rates, progressively decreases up to 0.7 at the lowest scan rate. In fact, Figure 5b and Figure 5c clearly illustrate the occurrence of a chemical reaction following the electron transfer. Assuming that a first-order chemical complication is operative, a lifetime $t_{1/2}$ of about 15 s can be assigned to [$Ru^{II}Cl_4$(DMSO)(Tz)]$^{2-}$. In addition, on the basis of the electrochemical reversibility of the electron transfer (ΔE_p constantly equal to the value of 59 mV theoretically expected for a one-electron process), it can be assumed that, before evolving slowly to the new species, [$Ru^{II}Cl_4$(DMSO)(Tz)]$^{2-}$ maintains the geometry of its Ru(III) precursor. Figure 5d finally confirms that the side product responsible for the spurious (starred) peak manifesting in the backscan at low scan rate becomes the predominant species after exhaustive reduction. As a consequence of the one-electron reduction, the original pale yellow solution (λ_{max} = 385 nm) becomes colorless (λ_{max} = 280 nm).

More intriguing appears the assignment of the second irreversible reduction. In this connection, Figure 6 compares the cyclic voltammetric behavior of [TzH][$RuCl_4$(DMSO)(Tz)] with that of [ImH][$RuCl_4$(DMSO)(Im)] (NAMI-A)[27] in aqueous solution. As seen, the imidazolate complex displays a first reduction exhibiting features quite similar to those of the thiazole complex (in fact, the trend of the current ratio with the scan rate is quite similar, as well as the spurious starred peak also appearing in the backscan), whereas the second reduction possesses features of partial chemical reversibility ($i_{pc}/i_{pa} = 0.7$ at 0.2 V s^{-1}).

It is noted that the use of a glassy carbon electrode causes in both the complexes the second cathodic process to shift very close to the solvent discharge. Such a finding not only allows one to rule out that such a process might be Ru-based but also supports the involvement of proton reduction.[28] In fact, it has been shown that Pt surfaces act as catalytic sites to favor the reduction of adsorbed H atoms to dihydrogen (with the extent of electrochemical reversibility decreasing with the increase of the pK_a of the different acids), whereas noncatalytic surfaces such as glassy carbon need large overpotentials. In support of such a proposal, in the case of [$(Im)_2$H][$Ru^{II}Cl_4$(Im)(NO)], an irreversible reduction around

(26) Brown, E. R.; Sandifer, J. R. *Phys. Methods Chem., Electrochem. Methods* **1986**, *2* (4).

(27) Alessio, E. Private communication.

(28) (a) Treimer, S. E.; Evans, D. H. *J. Electroanal. Chem.* **1998**, *39*, 449. (b) Treimer, S. E.; Evans, D. H. *J. Electroanal. Chem.* **1998**, *19*, 455. (c) Ferrali, M.; Bambagioni, S.; Ceccanti, A.; Donati, D.; Giorgi, G.; Fontani, M.; Laschi, F.; Zanello, P.; Casolaro, M.; Pietrangelo, A. *J. Med. Chem.* **2002**, *45*, 5776.

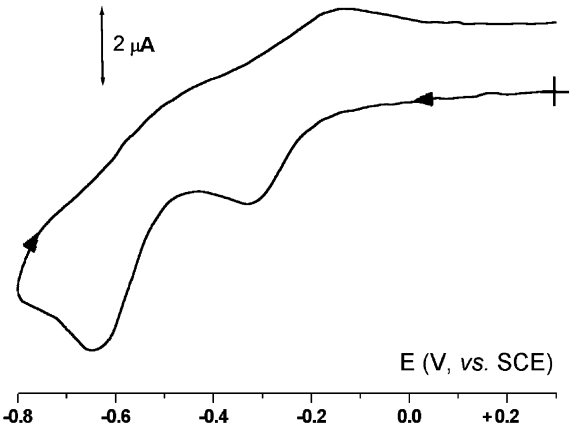

Figure 7. Cyclic voltammogram recorded at a platinum electrode in an aqueous solution of [TzH][$RuCl_4(Tz)_2$] (0.5×10^{-3} mol dm^{-3}). NaCl (0.2 mol dm^{-3}) supporting electrolyte. Scan rate 0.2 V s^{-1}.

−0.7 V (vs Ag/AgCl) in DMSO solution has been assigned to the reduction of the $[ImH]^+$ countercation.[29]

As far as the chemical complications following the first one-electron reduction are concerned, we recently found that in the cyclic voltammetric time scale the electrogenerated dianion $[Ru^{II}Cl_4(DMSO)(Im)]^{2-}$ undergoes replacement of the imidazole ligand for water, affording $[Ru^{II}Cl_4(DMSO)(H_2O)]^{2-}$. In turn, in the macroelectrolysis time scale, the further replacement of one chloride ligand occurs, affording $[Ru^{II}Cl_3(DMSO)(H_2O)_2]^-$.[30] In view of the similarity of the electrochemical responses, it does not seem ventured to assume that a similar path might hold for $[Ru^{II}Cl_4(DMSO)(Tz)]^{2-}$.

Since we are mainly interested in the Ru(III)/Ru(II) process, because of its biological implications, we will not dwell upon this topic further. We simply assume that the imidazolium ($pK_a \sim 7$) and thiazolium ($pK_a \sim 3$) cations might have different pK_a values, thus leading to different extent of reversibility of their proton reductions. Obviously, further investigations are needed to confirm the proposal.

As illustrated in Figure 7, a redox profile qualitatively similar to that of $[RuCl_4(DMSO)(Tz)]^-$ is displayed by $[Ru^{III}Cl_4(Tz)_2]^-$, but for the fact that the Ru(III)/Ru(II) process is significantly shifted toward more negative values, rather close to the assumed cation-centered irreversible reduction. Given the larger peak-to-peak separation and the lower current ratio of the latter, it can be assumed that the electrochemical reversibility of the electron transfer is lower (or, the reorganization energy higher) and the following chemical complication faster, respectively.

Table 4 compiles the formal electrode potentials of the Ru(III)/Ru(II) electron transfer for the mentioned derivatives.

Biological Properties. Some biological features of these ruthenium(III) thiazole complexes were preliminarily analyzed. Namely, we considered the following aspects: (i) the comparative binding abilities toward bovine serum albumin and calf thymus DNA and (ii) in vitro cytotoxicity against a reference human tumor cell line.

Table 4. Electrochemical Characteristics for the Redox Activity of the Ru(III) Complexes Here Studied in Aqueous NaCl Solution

complex	$E^{o\prime}$(Ru(III)/Ru(II)) (V vs SCE)	ΔE_p[a] (mV)	i_{pa}/i_{pc}[a]	E°(countercation reduction)[b] (V)	ref
$[Ru^{III}Cl_4(DMSO)(Tz)]^-$	+0.07	60	0.8	−0.62[a,c]	*d*
$[Ru^{III}Cl_4(DMSO)(Im)]^-$	0.00	80	0.8	−0.70[e]	*d*
$[Ru^{III}Cl_4(Tz)_2]^-$	−0.25	105	0.4	−0.65[a,c]	*d*
$[Ru^{III}Cl_4(Im)_2]^-$	−0.39	70	1		*f*

[a] Measured at 0.1 V s^{-1}. [b] See text. [c] Peak potential value for an irreversible reduction (see text). [d] Present work. [e] Partially chemically reversible reduction. [f] From ref 31.

Table 5. Results of Ultrafiltration Experiments

	[TzH][*trans*-$RuCl_4(Tz)_2$] (**I**)		[(TzH][*trans*-$RuCl_4(DMSO)(Tz)$]·(DMSO) (**II**)	
	BSA	DNA	BSA	DNA
up (%)	70	10	84	20
down (%)	30	90	16	80

Binding to Serum Albumin and Calf Thymus DNA. TzICR (**I**) and TzNAMI (**II**) were dissolved in the physiological buffer in the presence of equimolar amounts of either bovine serum albumin (BSA) or calf thymus DNA and the respective spectral profiles recorded over 24 h. The hydrolysis patterns of the two complexes, under these conditions, resemble closely those of the free complexes. Some differences are observed in the kinetics of these reactions. The spectral changes reach completion within 24 h.

The final samples were subjected to ultrafiltration to estimate the association of the ruthenium complexes to either serum albumin or calf thymus DNA. From the spectrophotometric analysis of the samples obtained after separation it is concluded that both complexes bind BSA tightly; at variance binding to calf thymus DNA is smaller. Results of ultrafiltration experiments are reported in Table 5.

Cytotoxicity. The cytotoxicity in vitro of both complexes was evaluated against the human tumor cell line A2780/S (ovarian carcinoma), using a single concentration of 50 μM. It is observed that such a relatively large concentration does not produce any significant inhibition of cell growth, implying that these complexes are virtually devoid of antiproliferative properties. This result correlates with previous results obtained on NAMI-A; in contrast, ICR had been previously reported to exhibit some cytotoxic effect at this concentration.

Discussion

Ruthenium(III) complexes are presently the object of great attention in the field of medicinal inorganic chemistry owing to the favorable pharmacological properties manifested by some members of this family of metallodrugs.[1] ICR and its indazole analogue KP1019, long investigated by the group of Bernhard Keppler, have demonstrated encouraging pharmacological properties and a low profile of toxicity. KP1019 has now entered phase I clinical trials.[2,3] Remarkably, the group of Trieste has shown that NAMI-A, a parent compound of ICR bearing a coordinated DMSO group in the place of

(29) Serli, B.; Zangrando, E.; Iengo, E.; Mestroni, G.; Yellowlees, L.; Alessio, E. *Inorg. Chem.* **2002**, *41*, 4033.
(30) Ravera, M.; Baracco, S.; Cassino, C.; Zanello, P.; Osella, D. Submitted.
(31) Ni Dhubhghaill, O. M.; Hagen, W. R.; Keppler, B. K.; Lipponer, K. G.; Sadler, P. J. *J. Chem. Soc., Dalton Trans.* **1994**, 3305.

an imidazole, exhibits outstanding antimetastatic properties on the Lewis lung tumor model. The cytotoxicity is low as well as the effects on the primary tumor. Notably, NAMI-A is presently undergoing advanced clinical tests.[4]

Thus, ruthenium complexes qualify as a peculiar family of antitumor agents with selective antimetastatic properties and low systemic toxicity. Yet, the molecular mechanism of action has not been elucidated. Also, no clear structure−function relationships have been established.

In the present paper we have prepared and characterized two novel ruthenium(III) complexes inspired by ICR and NAMI-A, that bear thiazole groups in the place of the imidazole groups of the parent compound.

These compounds have been studied both in the solid state and in solution. Structures in the solid state are very similar to those of the imidazole analogues; both complexes being characterized by a classical octahedral geometry, with four chlorides on the equatorial plane and the other groups in axial position.

The solution behavior of these ruthenium(III) thiazole complexes has been analyzed in detail. When dissolved in water, both complexes are sufficiently stable, at least for a few hours. At variance, upon dissolution in the reference phosphate buffer (pH 7.4), progressive, slow changes of the visible bands are observed that correlate to chloride hydrolysis. Notably, NAMI-A and TzNAMI, on one hand, and ICR and TzICR, on the other hand, exhibit great differences in their hydrolysis profiles, both in rates and shape. Indeed, the complexes bearing the DMSO ligand (NAMI-A and TzNAMI) are kinetically more labile than those containing two heteroaromatic groups; in turn, replacement of imidazole with thiazole results into a slowing of chloride release that is more marked in the case of TzNAMI. The appreciable stabilization of TzNAMI compared to NAMI-A might be advantageously exploited for clinical applications. Indeed, an overall encouraging pharmacological profile has been described very recently by the group of Trieste for TzNAMI.

The main electrochemical features of these compounds were analyzed in comparison to ICR and NAMI-A. Remarkably, TzNAMI shows oxidizing properties comparable to those of NAMI-A whereas TzICR manifests a lower propensitiy to undergo reduction in analogy with ICR. Since NAMI-A and ICR manifest significant differences in their pharmacological effects, one might argue that the biological differences are a consequence of the redox behavior and a similar situation seems to hold for their thiazole analogues.

Overall, the chemical characterization of the ruthenium(III) thiazole complexes supports the view that the presence of DMSO as a ligand confers specific properties to NAMI-A and TzNAMI compared to the TzICR and ICR complexes.

Beyond the structural and chemical characterization, we have reported here some additional experiments to elucidate a few biological aspects of these ruthenium(III) thiazole complexes. Specifically we have analyzed their cytotoxicity toward the human tumor cell line A2780/S and their comparative binding ability toward equimolar amounts of serum albumin and calf thymus DNA. Cytotoxicity experiments clearly revealed that both compounds are virtually noncytotoxic even at the highest tested concentrations, in line with expectations. In any case, the lack of cytotoxicity does not represent a clear drawback for the pharmaceutical applications of this family of compounds. Indeed, it is now well established that the favorable pharmacological properties of NAMI-A are unrelated to cytotoxicity: thus, NAMI-A represents a nice example of a promising antitumor drug that lacks cytotoxicity.

In the second series of experiments we analyzed comparatively the binding properties of the two complexes toward calf thymus DNA and serum albumin. Again, in line with previous results, we observed that binding to DNA is scarce for both complexes; in contrast relatively tight binding to serum albumin takes place. These result suggest that the mechanism of action of these ruthenium(III) complexes may differ largely from that of established platinum(II) complexes: DNA is likely not to represent the primary target so that alternative, protein-based targets should be considered.

Acknowledgment. We would like to thank CNR (Agenzia 2000) and CIRCMSB for the financial support.

Supporting Information Available: Crystallographic data in CIF format. This material is available free of charge via the Internet at http://pubs.acs.org.

IC0354116